JTTEE5 13:381-389
DOI: 10.1361/10599630420416
1059-9630/$19.00 © ASM International

Processing of Yttria Partially Stabilized Zirconia Thermal Barrier Coatings Implementing a High-Power Laser Diode

G. Antou, G. Montavon, F. Hlawka, A. Cornet, C. Coddet, and F. Machi

(Submitted September 3, 2003; in revised form October 27, 2003)

Several studies have been undertaken recently to adapt yttria partially stabilized zirconia (YPSZ) thermal barrier coating (TBC) characteristics during their manufacturing process. Thermal spraying implementing laser irradiation appears to be a possibility for modifying the coating morphology. This study aims to present the results of in situ (i.e., simultaneous treatment) and a posteriori (i.e., post-treatment) laser treatments implementing a high-power laser diode. In both cases, the coatings underwent atmospheric plasma spraying (APS). Laser irradiation was achieved using a 3 kW, average-power laser diode exhibiting an 848 nm wavelength. Experiments were performed to reach two goals. First, laser post-treatments aimed at building a map of the laser-processing parameter effects on the coating microstructure to estimate the laser-processing parameters, which seem to be suited to the change into in situ coating remelting. Second, in situ coating remelting aimed at quantifying the involved phenomena. In that case, the coating was treated layer by layer as it was manufactured. The input energy effect was studied by varying the scanning velocity (i.e., between 35 and 60 m/min), and consequently the irradiation time (i.e., between 1.8 and 3.1 ms, respectively). Experiments showed that coating thermal conductivity was lowered by more than 20% and that coating resistance to isothermal shocks was increased very significantly.

Keywords hybrid plasma spraying, isothermal shock resistance, laser remelting, thermal barrier coating, thermal conductivity, yttria partially stabilized zirconia

1. Introduction

1.1 Pore Network

Thermal spraying is a random deposition process during which molten particles impact at high velocity, spread, and solidify onto a substrate or previously deposited particles to form thin lamellae. The coating resulting from the stacking of those lamellae is characterized by a highly anisotropic lamellar structure. Moreover, stacking defects generate specific interlamellar features within the structure, mainly cavities (i.e., pores), which can be, or not, connected to the upper surface of the coating (i.e., open pores). Finally, vapors and gases stagnating in the vicinity of the surface to be coated and peripheral decohesions around lamellae induce, delaminations between the lamellae. In other respects, interlamellar microscopic cracks appear consecutively in the particle rapid solidification process after spreading. Such a phenomenon is especially emphasized for ceramic materials, which do not accommodate so much the shrinkage during the solidification. The combination of these features (Fig. 1) generates an interconnected network of pores, from which derives the permeability of most of the thermal spray coatings. This network can dramatically limit the coating in service performances, especially when the coated component is exposed to a reactive environment. In such a case, the substrate material reacts with the medium, which penetrates through the structure: corrosion occurs at the substrate/coating interface and eventually leads to the coating spallation.

1.2 Coating Post-Treatment

To circumvent the aforementioned difficulty, numerous approaches were scrutinized, such as (a) pore sealing by impregnation of organic or ceramic compounds,[1-3] or (b) structure remelting using in most cases an oxyacetylene flame and sometimes a laser beam.[4,5] This work deals with this latter approach. This article aims to present the results of in situ (i.e., simultaneous) and a posteriori (i.e., post-treatment) laser treatments. It focuses at first on the implemented process and its parameters. Then, coating microstructures resulting from these

Nomenclature	
APS	atmospheric plasma spraying
BC	bond coat
EBPVD	electron beam physical vapor deposition
OEM	original equipment manufacturer
PECVD	plasma-enhanced chemical vapor deposition
TBC	thermal barrier coating
TGO	thermally grown oxide
YPSZ	yttria partially stabilized zirconia

G. Antou, F. Hlawka, and **A. Cornet,** Laboratoire d'lngénierie des Surfaces de Strasbourg (LISS), Institut National des Sciences Appliquées (INSA) Strasbourg, 24 Blvd. de la Victoire, 67 000 Strasbourg, France; **G. Montavon** and **C. Coddet,** LERMPS, UTBM, 90 010 Belfort Cedex, France; and **F. Machi,** IREPA Laser, Parc Technologique, 67 400 Illkirch, France. Contact e-mail: ghislain.montavon@utbm.fr.

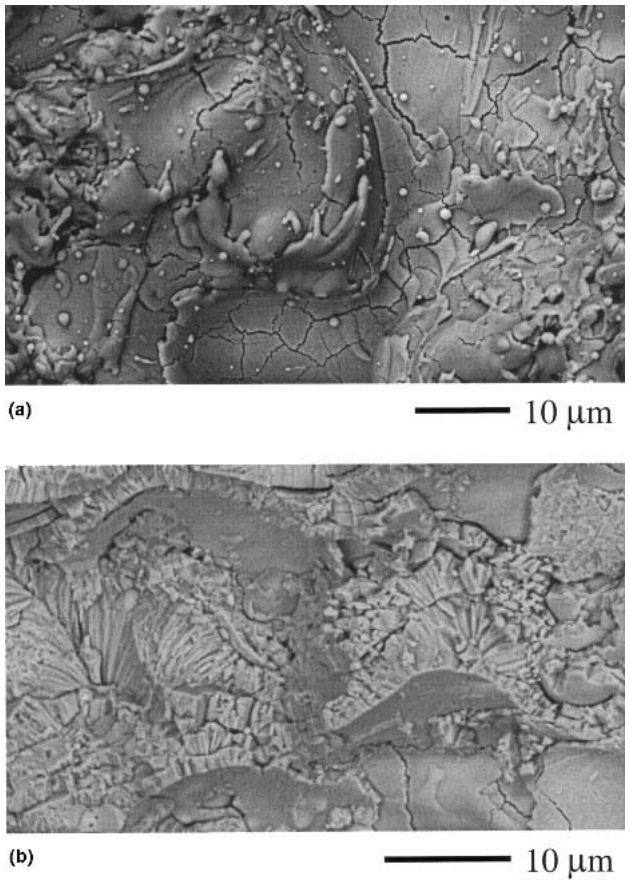

Fig. 1 Thermal spray ceramic coating **(a)** upper surface and **(b)** internal structure presenting cracks, decohesions, and pores constituting an interconnected pore network

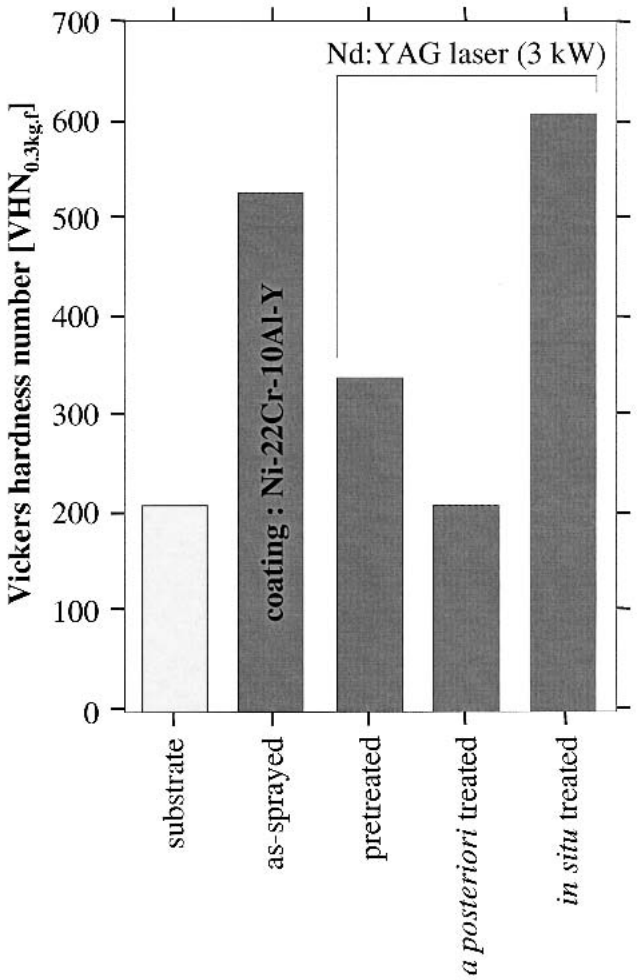

Fig. 2 Evolution of a NiCrAlY coating manufactured implementing various laser treatments, after the method of Eguchi et al.[6]

treatments are studied, and their thermal conductivity and their resistance to isothermal shocks are estimated.

1.3 Laser Remelting

Several studies have been undertaken in the past to modify thermal spray coating architecture implementing laser irradiation.[6-9] Whatever the nature of the treatment of the coating, the methodology was somehow the same. The first step consisted of manufacturing the coating via a classic route, and the second step consisted of post-treatment through its overall thickness. In such a case, the resulting microstructures were always made of fine columnar dendrites, but the rapid solidification (i.e., cooling rate ranging between 10^6 and 10^7 K/s[10]) of a large melting pool induced high levels of residual stresses, as well as numerous macroscopic cracks and delaminations affecting the structural cohesion. Consequently, such microstructures exhibit degraded physical properties, such as corrosion resistance and fatigue erosion resistance.[10]

To densify the structures without generating too high a level of cooling stresses, which would be incompatible with mechanical resistance properties, in situ coating remelting appeared to be an interesting alternative. This approach was never really investigated, except the very notable works performed in Japan by Eguchi et al.[6] This research team has clearly shown that in situ laser remelting of coating during their manufacture significantly enhanced their cohesion (Fig. 2).

1.4 Specific Case of Thermal Barrier Coatings

Thermal barrier coatings (TBCs) are widely used in gas turbines or diesel engines. Four primary constituents compose a thermal insulation system[11]:

- the ceramic top coat (i.e., the ceramic TBC), which is commonly manufactured using atmospheric plasma spraying (APS) process;
- the substrate materials, most commonly a superalloy;
- an aluminum-containing bond coat (BC) located between the metallic substrate and the ceramic TBC; and
- a thermally grown oxide (TGO), predominantly α-alumina,[12] that grows between the ceramic TBC and the BC.

The ceramic TBC behaves as the thermal insulator, the BC provides oxidation protection and behaves as a compliance layer, and the metallic substrate sustains the structural loads. The

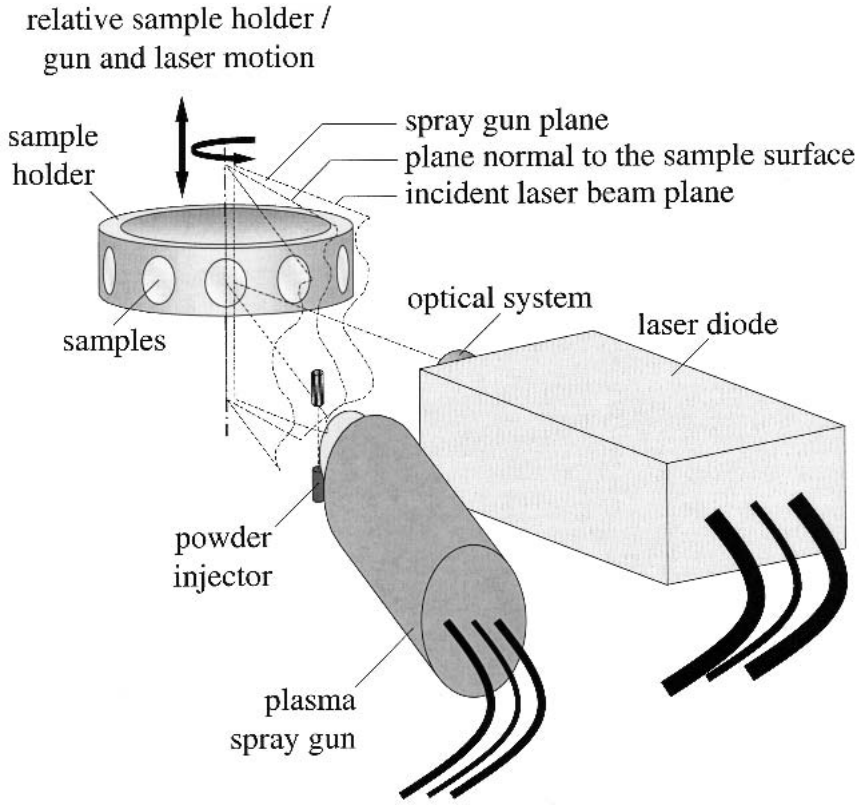

Fig. 3 Schematic of the experimental device

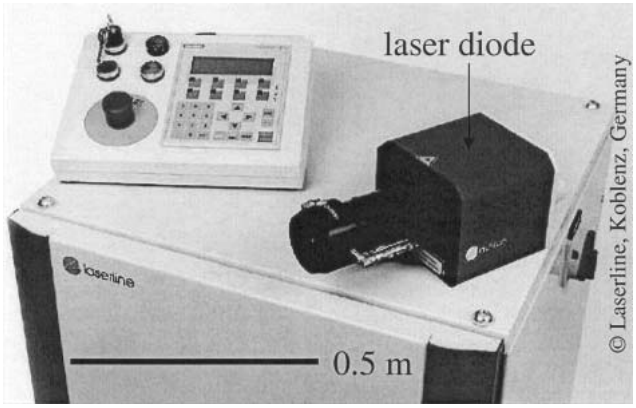

Fig. 4 The 3 kW laser diode used to perform these experiments

TGO is an oxidation reaction product that grows during the very first cycles of the system and plays a relevant role in the BC/TBC adhesion.[13] TBC systems exhibit several failure mechanisms,[13-18] which are generally attributed to (a) stress development during cooling after a high-temperature exposure and (b) a transient thermal stress appearance during rapid thermal cycling. In the first case, the TGO develops large compressive stresses upon cooling from operating temperatures, due to a substantial thermal expansion mismatch (i.e., on the order of 2.5-5 × 10^{-6}/K) with the underlying metallic substrate. In the second case, compressive stresses experienced by the plasma spray coating may cause the spalling (i.e., delamination) of individual lamellae. In any case, TBCs do not comply with high tensile stresses and relax by microcracking within their lamellar structure. Numerous studies during the last two decades have been undertaken to find ways to increase TBC characteristics. Among them, one can list:

- sealing of pores by impregnation of ceramic compounds;[1]
- plasma spraying under a low residual pressure (i.e., between 60 and 150 mbar) of a neutral atmosphere;[19] and
- altering the composition of the TBC by adding, for example, CeO_2, among other oxides, to improve phase stability, corrosion resistance, and thermal diffusivity properties.[20]

These approaches still remain palliative treatments and quite often induce one or even more additional steps in the manufac-

Table 1 Spray Parameters for YPSZ Used to Perform These Experiments

Parameter	Value
Arc current, A	630
Argon flow rate, SLPM[a]	44
Hydrogen flow rate, SLPM[a]	13
Feedstock carrier gas (argon) flow rate, SLPM[a]	3.4
Feedstock mass rate, g/min	15-25
Spray distance, mm	120
Spray velocity, m/min	30-60
Scanning velocity, mm/min	0.3-0.6

(a) SLPM, standard liter per minute

turing process. Thus, several studies[6-10] have been devoted to adapting TBC characteristics during their manufacturing process. Thermal spraying combined with laser irradiation to induce the remelting of structures appears to be one of the possibilities.

2. Experimental Protocol

2.1 Feedstock

Yttria (7% wt.%) partially stabilized zirconia (YPSZ) was chosen as the feedstock material for conducting in situ remelting treatments. The 204B-NS powder (Sulzer-Metco, Wohlen, Switzerland) was selected, as this feedstock complies with numerous original equipment manufacturer (OEM) specifications, being primarily used as TBCs for turbine combustion liners and airfoils. The feedstock exhibited a particle size distribution ranging from 45-75 μm, with hollow particle architecture.

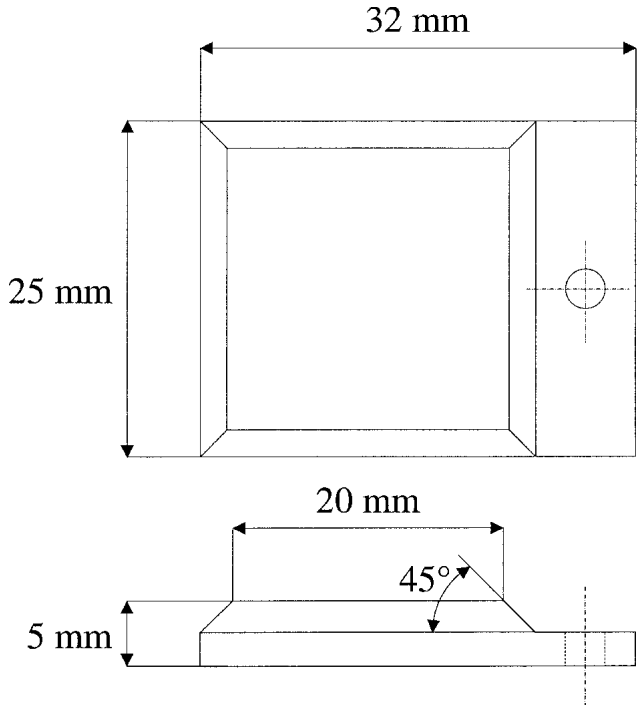

Fig. 5 Substrate shape used for the cyclic isothermal shock test[21]

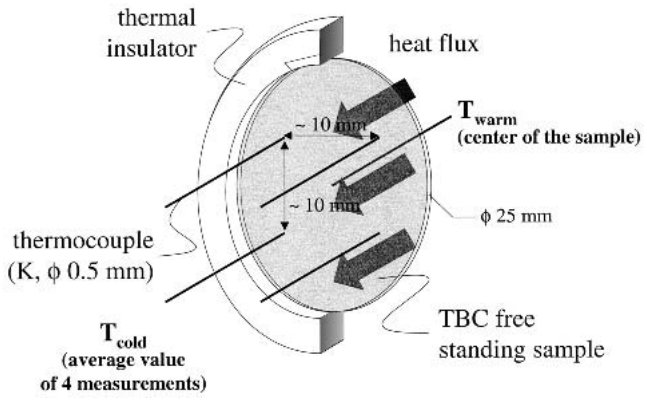

Fig. 6 Schematic experimental device for thermal conductivity measurements

2.2 Experimental Device

The experimental device (Fig. 3) consisted of the association of an F4 direct current (dc) plasma spray gun from Sulzer-Metco and a high-power laser diode of 3 kW average power, exhibiting an 848 nm wavelength, from Laserline (Koblenz, Germany) (Fig. 4). The choice of such a type of laser presents numerous advantages. Among them, its compactness, which permits the easy integration of the laser within the spray environment, and its wavelength, which permits an increase in laser absorption by the matter, are among the most noticeable.

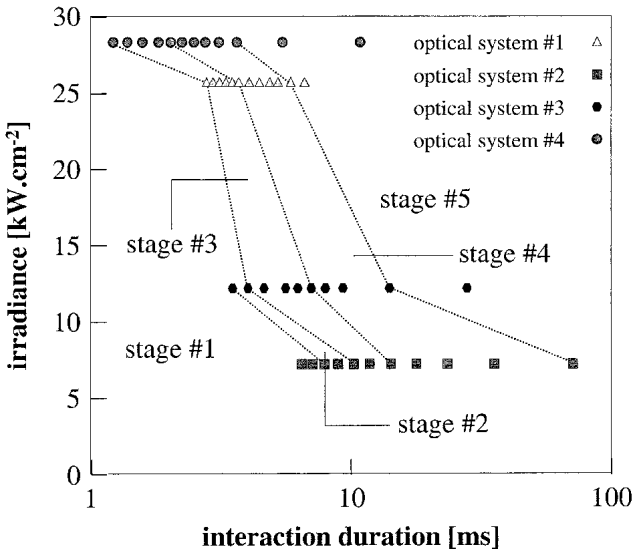

Fig. 7 Process map: evolution of the melting state as a function of the irradiance and the interaction time, for various optical systems. Dashed lines delineated approximately the different melting stages.

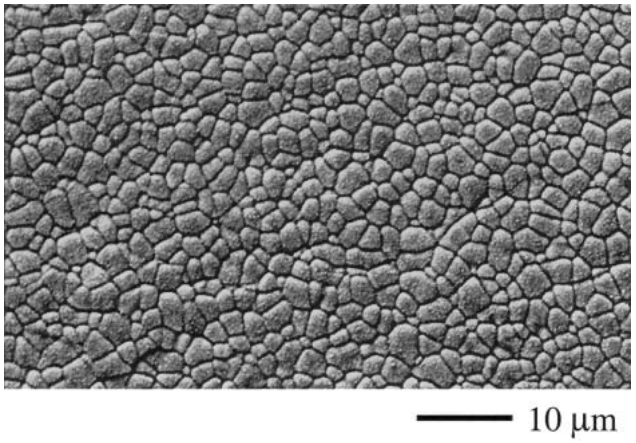

Fig. 8 Typical upper surface morphology of a YPSZ remelted coating

2.3 Processing Parameters

YPSZ coatings were sprayed onto low-carbon steel coupons 25 mm in diameter and 25 mm in thickness. The spray parameters for YPSZ are listed in Table 1. The feedstock mass rate was adjusted consequently to the spray velocity, which itself depended on the selected laser irradiance, to ensure a constant deposited thickness per pass of about 12-15 μm. Two types of experiments were carried out:

- laser post-treatments aimed at defining a map of the processing parameter effects on the coating microstructure to estimate laser parameters for in situ processing of coatings; and
- in situ coating remelting to quantify the involved phenomena. In this latter case, the coatings were remelted layer by layer, as they were manufactured.

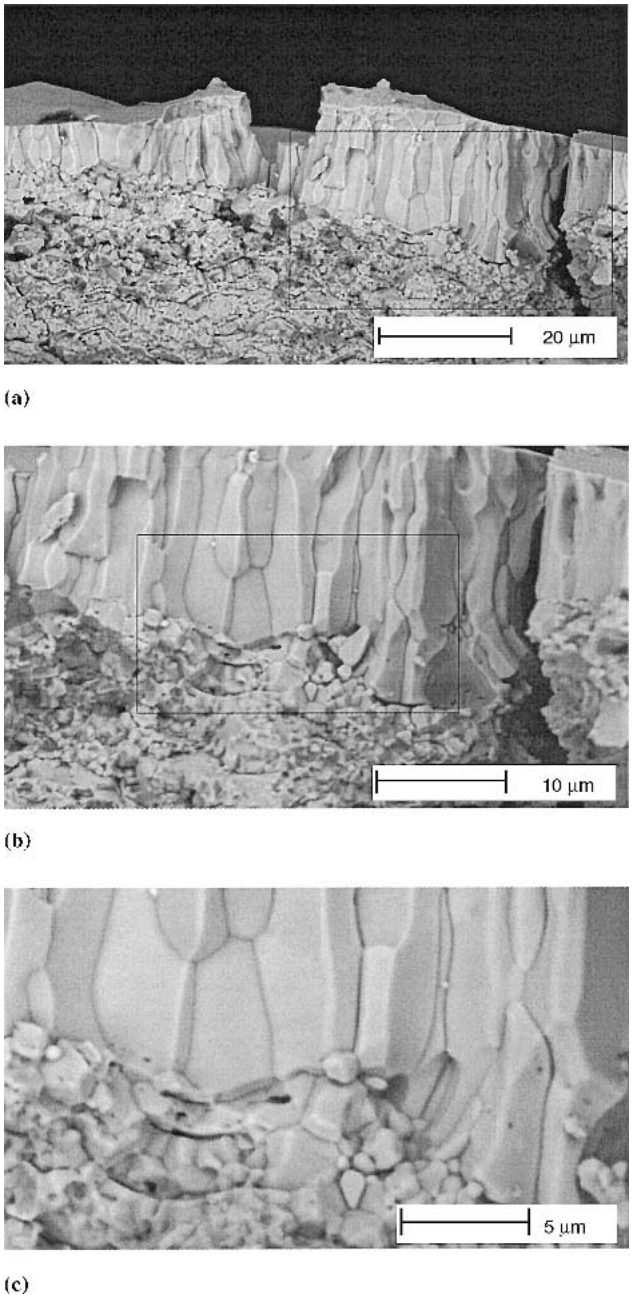

Fig. 9 Columnar structure of a YPSZ in situ remelted layer on top of as-sprayed layers: **(a)** 20 μm; **(b)** 10 μm; **(c)** 5 μm

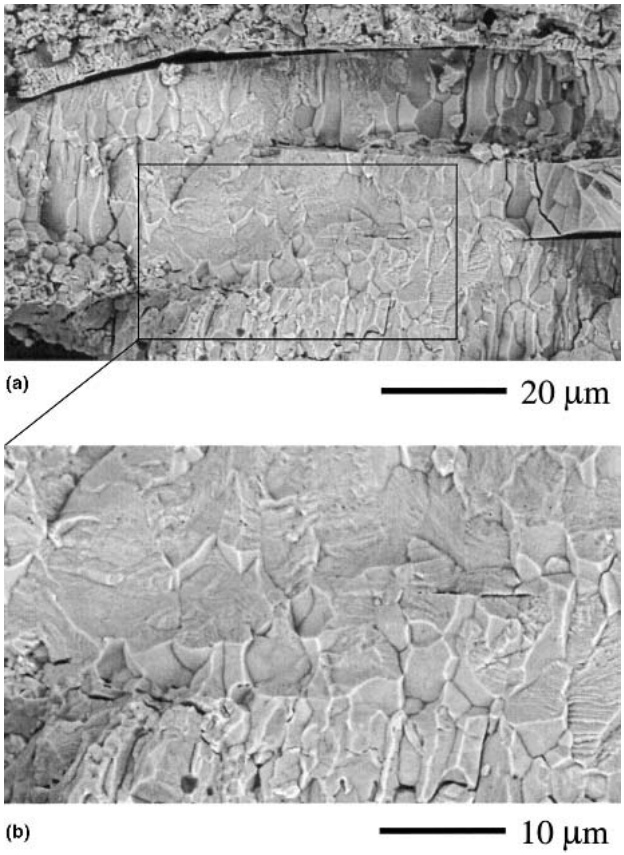

Fig. 10 Interface between successive in situ remelted layers of a YPSZ coating: **(a)** 20 μm; **(b)** 10 μm

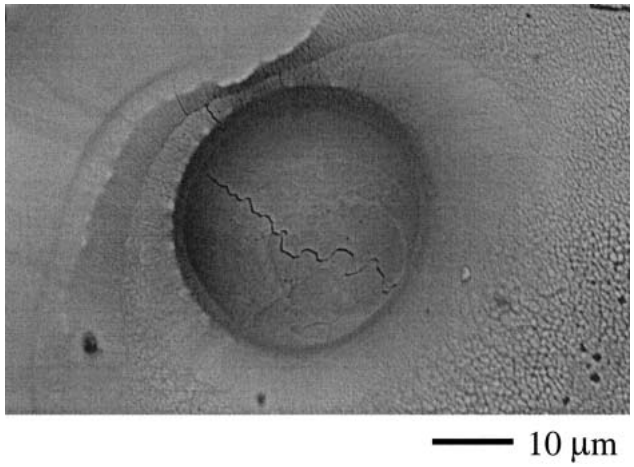

Fig. 11 Detail of preferential remelting around singularities of the YPSZ coating surface

Concerning laser post-treatment, the map of the laser-processing parameter effects was studied implementing four optical systems, which permitted evaluation of the influence of irradiation time and input energy on the resulting molten state. To conduct in situ laser remelting tests, the input energy effects were studied by varying the spray velocity (i.e., from 35-60 m/min), and consequently the irradiation duration (i.e., from 1.8-3.1 ms, respectively) using one optical system.

2.4 Sample Characterization

Samples were sectioned to coupons using a diamond saw in an oil medium. The coupons were then impregnated and mounted onto rings using an epoxy resin. Coupons were polished using an automatic polisher (Vanguard, Buehler, Lake Bluff, IL) to get reproducible results and were observed either by optical or scanning electron microscopy. Samples were also cooled down in liquid nitrogen and broken to observe the failure facieses.

2.5 Cyclic Isothermal Shock Test

To investigate the thermal behavior of the treated coatings, cyclic isothermal shock test was carried out. Samples were 20 × 20 mm square and 5 mm thick,[21] and were made of the same low-carbon steel (Fig. 5). They were sprayed following the same protocols. The coated specimens were kept in a furnace for 10 min at the test temperature of 1273 K and then were dropped into icy water (279 ± 2 K). After each thermal cycle, the sample was visually inspected. The test was interrupted when the TBC coat spalled from more than 50% of the test zone. One sample per process parameter set was tested.

2.6 Thermal Conductivity Measurement

Thermal conductivity measurement was conducted to evaluate the influence of laser remelting on the thermal conduction through TBCs. One sample per process parameter set was tested. The protocol was as follows (Fig. 6).

1. To put a free-standing TBC in front of radiation emitted by a warm source of about 773 K. Samples were insulated to stay in the case of a monodimensional heat conduction. Warm temperature (T_{warm}) and cold temperature (T_{cold}) were measurements were taken from five thermocouples, with T_{cold} being the average of four measurements.
2. To determine the thermal flux through the sample. The test used in this case a fully oxidized copper chip of 3 mm thickness with a surface roughness equivalent to that of the remelted YPSZ coatings (i.e., about 1.6 μm average roughness). Hence, knowing the thermal conductivity of copper (about 377 W/m · K between 0 and 773 K[22]), the thermal flux was calculated according to the Fourier first law. Effectively, the hemispherical spectral emissivities between 2 and 10-12 μm for the wavelengths of oxidized copper and YPSZ TBC are equivalent in a rough approximation[23,24] that is the heat fluxes through the copper disk and through the ceramic disks can be equated in a first approximation.
3. Finally, knowing T_{warm} and T_{cold}, the thermal flux through the sample, and the sample thickness (measured by image analysis), the thermal conductivity of each sample could be calculated according to the Fourier first law.

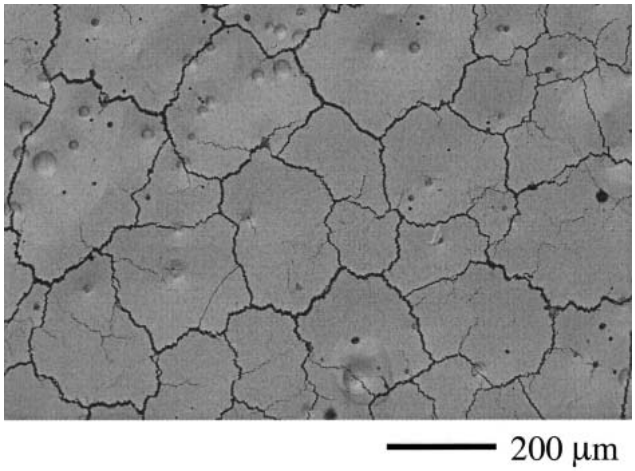

Fig. 12 Crack network in the remelted zone

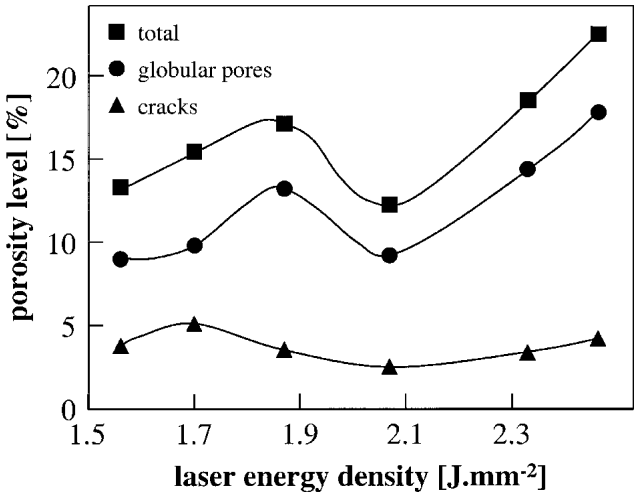

Fig. 13 Evolution of the porosity level as a function of the laser energy density

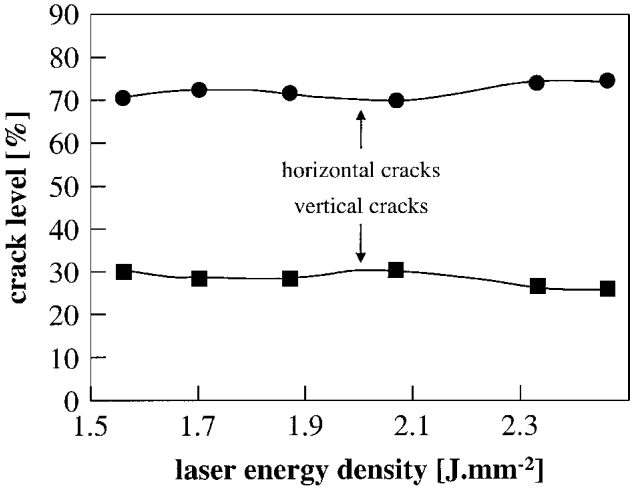

Fig. 14 Crack orientation as a function of the laser energy density

3. Results and Analysis

3.1 Process Map

Sample facies manufactured implementing laser post-treatments were qualified to build the laser treatment process map for YPSZ, which is valuable for targeting suitable in situ treatment parameters. The effects of the laser irradiation on the deposit morphologies were qualified, using stereoscopic micrography, for several sets of processing parameters, as follows:

- stage 1: no detectable molten zone; treated area exhibiting the same aspect as the as-sprayed deposits;
- stage 2: no detectable molten zone; treated area exhibiting a different aspect (i.e., a different color);
- stage 3: localized molten zones;
- stage 4: continuous molten zones; and
- stage 5: continuous molten zones; the substrate is detectable under the YPSZ by transparency.

Figure 7 presents the map of laser-processing parameter effects (i.e., irradiance versus interaction duration). From a general point of view, the molten state depends on the laser irradiation energy (i.e., on the irradiance and on the interaction duration). Moreover, it seems to become critical to obtain continuous melted zones (i.e., stages 4 and 5) for irradiation energy lower than 0.5 J/mm^2.

3.2 Coating Structure

The microstructure resulting from laser treatment is a columnar dendritic structure (Fig. 8). The characteristic dimension of the columnar grains ranges from 1-3 μm, average diameter, for laser post-treatment, and from 0.5-1 μm, average diameter, for in situ laser remelting. As the solidification is directional, the microstructure orientation is directional, and this microstructure orientation is due to the positive temperature gradient from the substrate to the remelted area. In the case of in situ laser remelting, the microstructure refinement could be explained by a higher temperature reached at the end of the remelting compared with laser post-treatment. Figure 9 illustrates the columnar structure, at various magnifications, of a YPSZ in situ remelted layer on top of as-sprayed layers. Among various features, the interface between the columnar and the layered structures (i.e., remelted and as-sprayed structures, respectively) seems quite good with no visible decohesion at the interface. Figure 10 illustrates the interface between two successive in situ remelted layers of the YPSZ coating. The quality of the interface is quite high, with a continuity of the columnar structure through the layers. However, some decohesions remain.

3.3 Specific Features

Some laser parameters induced inhomogeneous coating treatments. Molten zones appeared preferentially near surface singularities and were typified by the formation of cavities (Fig. 11). The origin of this localized remelting could be attributed to:

- open pores, which behave like thermal pools. It is very likely that the molten areas expand in this case by thermal conduction;
- impurities within the coating exhibiting lower melting temperatures or higher absorption coefficients than YPSZ; and
- gas pockets, which make their way toward the surface, via liquefaction and suddenly release in the atmosphere.

3.4 Crack Network

With regard to laser post-treatment, the remelted layers, homogeneous or not, are characterized by a crack network (Fig. 12). As a matter of fact, when the laser energy is raised, the remelted thickness increases and varies from 9-60 μm, from the lowest to the highest laser energy density (i.e., from 0.5-9.9 J/mm^2, respectively). Consequently, the volume reduction consecutive to solidification is higher, and this induces the generation of high levels of residual stresses within the structure: vertical cracking, perpendicular to the substrate surface, then occurs when the local mechanical resistance of the coating is reached. Besides, delaminations appear near the substrate/coating interface as soon as the remelted thickness becomes higher than 10-15 μm, (i.e., for a laser energy higher than 0.8 J/mm^2). Such a phenomenon is very likely induced by the thermal expansion mismatch between the substrate and the coating that also generates stresses.[8] Concerning in situ laser remelting, vertical cracking is far less emphasized. This could be simply explained, in a first approximation, by the lower required energy, which hence lowers the thermal shock.

Two types of porosity were distinguished by image analysis[25]: (a) the globular porosity, which corresponds to pores of about 10 μm diameter; and (b) the microcracks. Figure 13 displays the evolution of the porosity level as a function of the laser energy density. Whereas the porosity level linked to microcracks is stable at around 4-5%, it clearly appears that the total porosity increases from about 14-15% to 20% for a laser energy higher than 2.2 J/mm^2. This is directly related to an enhancement of the globular porosity. As a matter of fact, when the laser energy reaches high levels, thermal shocks and remelted thicknesses increase. This induces the formation of large cracks in the deposit. Concerning the crack network orientation, horizontal and vertical cracks were discerned.

Whatever the laser energy density, the proportion is always the same: one-third of vertical cracks and two-thirds of horizontal cracks (Fig. 14). For low laser energy densities, this seems to be linked to the lamellar structure of the coating and the resulting interlamellar decohesions. For higher laser energy density, the crack distribution is certainly more related to the fact that the thermal expansion mismatch between the BC and the ceramic creates stresses in the deposit and, hence, induces the formation of horizontal cracks (i.e., delaminations).

3.5 Isothermal Shock Resistance of In Situ Remelted Coating

Evans et al.[26] has shown that the main degradation mechanism during isothermal shocks is the growth of the TGOs. (1) separations are induced into the coating, (2) the separations propagate around imperfections induced in the TGO, and, finally, (3) coalesce and become large enough to satisfy large buckling. This is the observed mechanism operating during these isothermal shocks (Fig. 15).

Figure 16 shows the evolution of the number of cyclic isothermal shocks inducing a spallation of 50% of the coated surface of in situ remelted coatings for various laser energy densi-

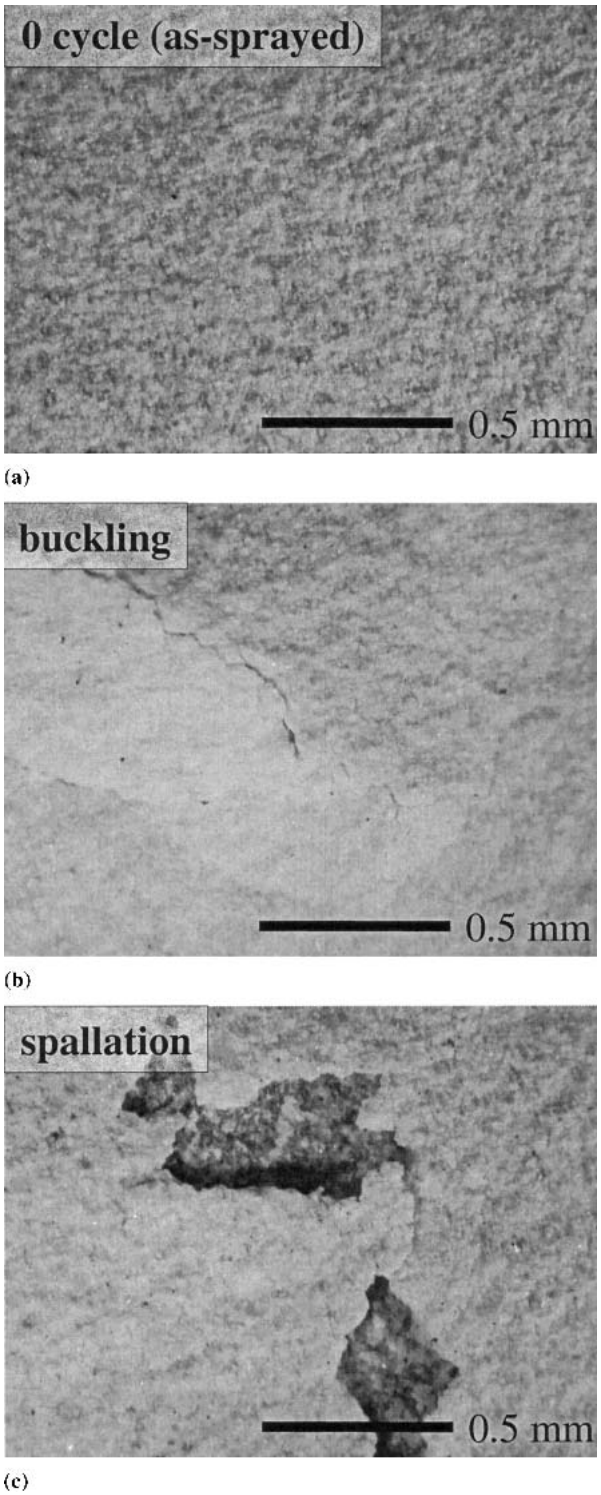

Fig. 15 Observed degradation mechanism during isothermal shocks: **(a)** 0 cycle (as-sprayed); **(b)** buckling; **(c)** spallation

ties. It clearly appears that in situ remelted coatings exhibit better resistance to isothermal shocks than as-sprayed coatings. The resistance to isothermal shocks is even increased two-fold for a laser energy density of 1.7 J/mm^2. This shows that the columnar structure and the pore-crack architecture of the remelted coating improve the compliance property and decrease the permeability of TBCs.

3.6 Thermal Conductivity

Figure 17 displays the evolution of the thermal conductivity of in situ remelted and as-sprayed coatings as a function of laser energy density. A decrease of about 20% of the thermal conductivity was obtained for the laser-treated coating. The thermal conductivity of a remelted coating is about 0.6-0.7 W/m · K. This constitutes a very promising result, and it seems to be linked to the existence of horizontal cracks into the in situ remelted coatings, which behave as thermal resistances. These horizontal cracks appear between the remelted layer and the as-sprayed layer. It can be explained by the fact that, as the remelted layer is smooth, the as-sprayed layer does not adhere very well to it.

4. Conclusion

Laser treatment is considered as a technique to densify thermal spray coatings. This study consisted of remelting YPSZ coatings, using a 3 kW, average-power, diode laser to explore especially the possibilities of in situ treatments and to investigate laser-processing parameter effects on the morphology of YPSZ coatings.

In situ laser remelting has very heightened effects on YPSZ plasma-sprayed structures. As a matter of fact, the association of a high-power laser diode with a spray gun permitted the authors to:

- modify the lamellar structure of the as-sprayed coating to a columnar dendritic structure;
- achieve a columnar structure that presents an elastic behavior similar to that of the bulk material of the as-sprayed coating;
- increase twofold the lifetime of TBCs during isothermal shock tests; and
- decrease by about 20% their thermal conductivity.

Hence, in situ remelting of plasma-sprayed YPSZ TBCs enabled thermal conductivity as low as 0.6-0.7 W/m · K, whereas plasma spraying permitted us to reach thermal conductivity of about 1-1.3 W/m · K, electron beam physical vapor deposition

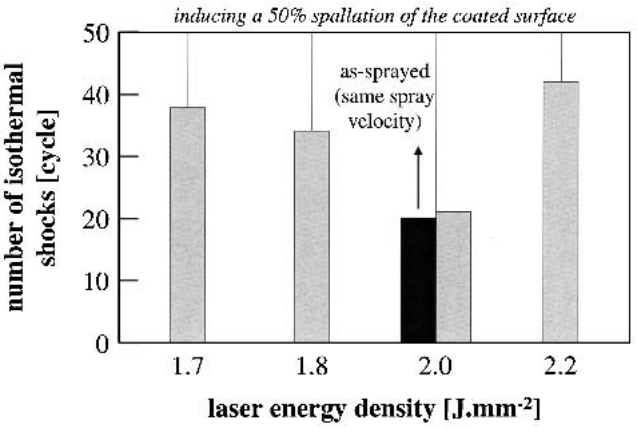

Fig. 16 Results of isothermal shocks carried out on as-sprayed and in situ remelted samples

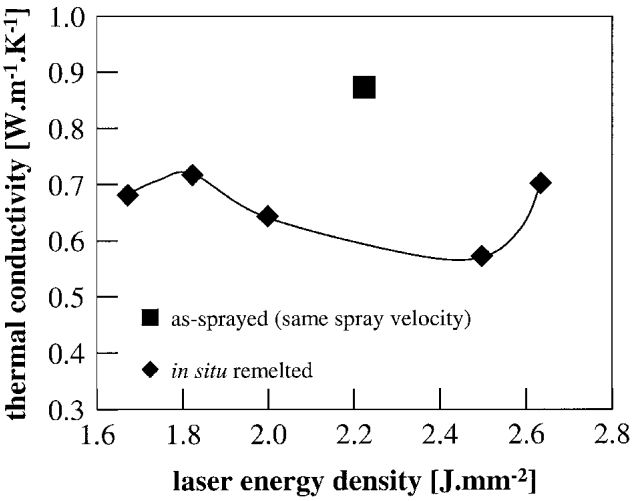

Fig. 17 Results of thermal conductivity measurement carried out on as-sprayed and in situ remelted samples

(EBPVD) enabled thermal conductivity of about 1.5-1.8 W/m · K, and plasma-enhanced chemical vapor deposition (PECVD) permitted us to reach thermal conductivity of about 1.5-2 W/m · K.[27-29]

Acknowledgments

The authors gratefully acknowledge F. Pandrak and L. Lahoupe from Laboratoire d'Etudes et de Recherches sur les Matériaux, les Procédés et les surfaces (LERMPS)-Université de Technologie de Belfort-montbéliard (UTBM) for their valuable helps. LERMPS is a member of the Institut des Traitements de Surface de Franche-Comté (ITSFC, Surface Treatment Institute of Franche-Comté), France.

References

1. R.T. Lahtinen and P.J.T. Jokinen: "Painting of Arc Sprayed Zinc Coatings With Water-Based Paints" in *Thermal Spray: Surface Engineering via Applied Research,* C.C. Berndt, ed., ASM International, Materials Park, OH, 2000, pp. 1077-80.
2. S. Ahmaniemi, E. Rajamäki, P. Vuoristo, and T. Mäntylä: "Effect of Aluminum Phosphate Sealing Treatment on Properties of Thick Thermal Barrier Coatings" in *Thermal Spray: Surface Engineering via Applied Research,* C.C. Berndt, ed., ASM International, Materials Park, OH, 2000, pp. 1081-86.
3. Y. Kimura, Y. Yoshioda, and M. Kanazawa: "On the Effects of Sealing Treatment and Micro-Structural Grading Upon Corrosion Characteristics of Plasma-Sprayed Ceramic Coating" in *Thermal Spray Industrial Applications,* C.C. Berndt and S. Sampath, ed., ASM International, Materials Park, OH, 1994, pp. 527-32.
4. L. Pawlowski: "Laser Treatment of Thermally Sprayed Coatings" in *Conference Proceedings of 2002 International Thermal Spray Conference,* E. Lugscheider, ed., DVS-German Welding Society, Düsseldorf, Germany, 2002, pp. 721-26.
5. S.O. Chwa and A. Ohmori: "Observation of Microstructure in Thermal Barrier Coatings Prepared by Laser Hybrid Spraying Process Using Fluorescent Dye Infiltration Technique" in *Conference Proceedings of 2002 International Thermal Spray Conference,* E. Lugscheider, ed., DVS-German Welding Society, Düsseldorf, Germany, 2002, pp. 253-57.
6. N. Eguchi, H. Shirasawa, and A. Ohmori: "NiCrAlY Coatings in YAG laser Combined Low Pressure Plasma Spraying" in *Thermal Spray: Meeting the Challenges of the 21st Century,* C. Coddet, ed., ASM International, Materials Park, OH, 1998, pp. 1517-22.
7. G. Montavon and C. Coddet: "Modification of Ceramic Thermal Spray Coating Implementing Laser Treatment" in *Thermal Spray 2001: New Surfaces for a New Millennium,* C.C. Berndt, K.A. Kohr, and E. Lugscheider, ed., ASM International, Materials Park, OH, 2001, pp. 1195-1202.
8. S. Nowotny, S. Scharek, R. Zieris, T. Naumann, and E. Beyer: "Innovations in Laser Cladding," *Laser Mater. Proc.,* 2000, *89,* pp. 11-15.
9. Y. Yuanzheng, Z. Youlan, L. Zhengyl, and C. Yuzhi: "Laser Remelting of Plasma Sprayed Al_2O_3 Ceramic Coatings and Subsequent Wear Resistance," *Mater. Sci. Eng.,* 2000, *A291,* pp. 168-72.
10. L. Pawlowski: "Thick Laser Coatings: a Review," *J. Thermal Spray Technol.,* 1999, *8*(2), pp. 279-95.
11. D. Stöver and C. Funke: "Directions of the Development of Thermal Barrier Coatings in Energy Applications," *J. Mater. Proc. Technol.,* 1999, *92-93,* pp. 192-202.
12. K. Ogawa, T. Masuda, and T. Shoji: "Kinetic of Thermally Grown Oxide at Interface between Thermal Barrier Coatings and MCrAlY Bond Coatings" in *Thermal Spray 2001: New Surfaces for a New Millennium,* C.C. Berndt, K.A. Kohr, and E. Lugscheider, ed., ASM International, Materials Park, OH, 2001, pp. 187-94.
13. D.R. Mumm, A.G. Evans, and I.T. Spitsberg: "Characterization of a Cyclic Displacement Instability for Thermally Grown Oxide in a Thermal Barrier System," *Acta Mater.,* 2001, *49,* pp. 2329-40.
14. J. Rösler, M. Bäker, and M. Volgmann: "Stress State and Failure Mechanisms of Thermal Barrier Coating: Role of Creep in Thermally Grown Oxide," *Acta Mater.,* 2001, *49,* pp. 3659-70.
15. M.Y. Ali, S.Q. Nusier, and G.M. Newaz: "Mechanics of Damage Initiation and Growth in a TBC/Superalloy System," *Int. J. Solids Struct.,* 2001, *38,* pp. 3329-40.
16. P. Nylen, M. Friis, A. Hansbo, and L. Pejryd: "Investigation of Particle In-Flight Characteristics During Atmospheric Plasma Spraying of Yttria Stabilized ZrO2: Part 2. Modeling," *J. Thermal Spray Technol.,* 2001, *10*(2), pp. 359-66.
17. V. Teixeira, M. Andritschky, H. Gruhn, W. Mallener, H.P. Buchkremer, and D. Stöver: "Failure of Physical Vapor Coatings/Plasma-Sprayed Thermal Barrier Coatings During Thermal Cycling," *J. Thermal Spray Technol.,* 2000, *9*(2), pp. 191-97.
18. J.A. Haynes, E.D. Rigney, M.K. Ferber, and W.D. Porter: "Oxidation and Degradation of Plasma-Sprayed Thermal Barrier Coating System," *Surf. Coat. Technol.,* 1996, *86-87,* pp. 102-108.
19. H.D. Steffens, J. Wilden, and T. Duda: "Thermal Spraying," *J. High Temp. Chem. Proc.,* 1994, *3*(6), pp. 653-64.
20. C.H. Lee, H.K. Kim, H.S. Choi, and H.S. Ahn: "Phase Transformation and Bond Coat Oxidation Behavior of Plasma-Sprayed Zirconia Thermal Barrier Coating," *Surf. Coat. Technol.,* 2000, *124,* pp. 1-12.
21. S.O. Chwa and A. Ohmori: "Microstructures of ZrO_2-8 Y_2O_3 Coatings Prepared by a Laser Hybrid Spraying Technique," *Surf. Coat. Technol.,* 2002, *153,* pp. 304-12.
22. J. Barbery: "Numerical Data on Copper and Welded Alloys," in *Techniques de l'Ingénieur,* Les Techniques de l'Ingénieur, Paris, France, 1998, pp. M433.1-M433.68.
23. R. Siegel and J.R. Howell: *Thermal Radiation Heat Transfer,* 4th ed., Taylor and Francis, New York, NY, 2002, p. 112.
24. C.H. Liebert: "Emittance and Absorptance of NASA Ceramic Thermal Barrier Coating System," NASA Technical Paper 1190, 1978, National Aeronautics and Space Administration, p. 26.
25. G. Antou, G. Montavon, F. Hlawka, A. Cornet, C. Coddet, J. Staerck, and O. Frénaux: "Analysis of Pore Connectivity Modification and Structure Densification of Y-PSZ Coatings After In Situ Laser Remelting Implementing Electrochemical Test" in *Thermal Spray 2003: Advancing the Science & Applying the Technology,* C. Moreau and B. Marple, ed., ASM International, Materials Park, OH, 2003, pp. 1507-11.
26. A.G. Evans, D.R. Mumm, J.W. Hutchinson, G.H. Meier, and F.S. Pettit: "Mechanisms Controlling the Durability of Thermal Barrier Coatings," *Prog. Mater. Sci.,* 2001, *46,* pp. 505-53.
27. D.D. Hass, A.J. Slifka, and H.N.G. Wadley: "Low Thermal Conductivity Vapor Deposited Zirconia Microstructures," *Acta Mater.,* 2001, *49,* pp. 973-83.
28. J.R. Nicholls, K.J. Lawson, A. Johnstone, and D.S. Rickerby: "Methods to Reduce the Thermal Conductivity of EBPVD TBCs," *Surf. Coat. Technol.,* 2002, *151-152,* pp. 383-91.
29. B. Préauchat and S. Drawin: "Isothermal and Cycling Properties of Zirconia-Based Thermal Barrier Coatings Deposited by PECVD," *Surf. Coat. Technol.,* 2001, *146-147,* pp. 94-101.